Structural, electronic and optical properties of orthorhombic distorted perovskite $TbMnO_3$*

Cai Lu-Gang(蔡鲁刚), Liu Fa-Min(刘发民)†, and Zhong Wen-Wu(钟文武)

Department of Physics, School of Physics and Nuclear Energy Engineering, Key Laboratory of Micro-nano Measurement-Manipulation and Physics (Ministry of Education), Beijing University of Aeronautics and Astronautics, Beijing 100191, *China*

(Received 1 February 2010; revised manuscript received 18 March 2010)

This paper calculates the structural parameters, electronic and optical properties of orthorhombic distorted perovskite-type $TbMnO_3$ by first principles using density functional theory within the generalised gradient approximation. The calculated equilibrium lattice constants are in a reasonable agreement with theoretical and experimental data. The energy band structure, density of states and partial density of states of elements are obtained. Band structures show that $TbMnO_3$ is an indirect band gap between the O 2p states and Mn 3d states, and the band gap is of 0.48 eV agreeing with experimental result. Furthermore, the optical properties, including the dielectric function, absorption coefficient, optical reflectivity, refractive index and energy loss spectrum are calculated and analysed, showing that the $TbMnO_3$ is a promising dielectric material.

Keywords: density functional theory, band structure, density of states, optical property

PACC: 7115, 7820

1. Introduction

Multiferroics, materials combining the characteristics of ferroelectric and ferromagnetic order, have attracted extensive attention in the condensed matter physics and material science.[1−5] One of the hot topics in multiferroics is the magnetoelectric effect, that is, the spontaneous electric polarisation induced by external magnetic field and the magnetization induced by external electric field. The coexistence of electric polarisation and magnetization, especially the magnetoelectic coupling, has fundamental importance for applications in devices, such as disk memory.[6] Both experimental and theoretical methods have been reported extensively for the research in mutiferroics.[7,8] Among the multiferroics, ABO_3, the transition metal oxides is a main research area due to the easy mutual controlling between ferroelectric and magnetoelectric states, where B usually represents transition-metal ions, such as Fe, Mn.[9,10] The quest for understanding the origin of the multiferroicity has stimulated a great interest in the magnetic, structural, and dielectric properties for multiferroic materials. In the present work, we will report the electric structure and optical properties based on the first-principle calculation, and take $TbMnO_3$ as an example.

$TbMnO_3$ is by far one of the most studied multiferroic manganeses and exhibits an orthorhombic distorted perovskite structure with *Pbnm* symmetry containing a network of corner-sharing MnO_6 octahedron.[11,12] The neutron diffraction has revealed that the manganite undergoes a phase transition into an sinusoidal anti-ferromagnetic (AFM) collinear spin structure at the Nĕel temperature ($T_N = 42$ K) and subsequently into a structure with cycloidal spin order and an spontaneous electric polarisation along the c axis emerges simultaneously at $T_{FE} = 27$ K.[13] Especially, the electric polarisation can be switched from the direction along the c axis to that along the a axis when tuning the magnitude of magnetic field along the b axis below the temperature of $T_{FE} = 27$ K. The mechanism of the relation between the electric polarisation and the magnetic moments has well explained in a system with spiral magnetic structures from symmetry consideration, described by the equation of $\boldsymbol{P} \sim \boldsymbol{e}_{ij} \times (\boldsymbol{S}_i \times \boldsymbol{S}_j)$, with $\boldsymbol{e}_{ij}$ being the unit vector connecting magnetic moments at i and j.[14]

Until now, extensive studies have been done for ferroelectric and ferromagnetic properties. And Li *et al.* have presented some reports for some ABO_3

*Project supported by the Financial Support from Equipment Research Foundation of China (Grant No. 373974).

†Corresponding author. E-mail: fmliu@buaa.edu.cn

© 2010 Chinese Physical Society and IOP Publishing Ltd

materials.[15−18] In order to fully take advantage of the properties of $TbMnO_3$ for an eventual technological application, a theoretical investigation of the structural, electronic and optical properties is necessary. In the present work we report a first-principle study of physical properties of $TbMnO_3$ in the limit of very low temperature (normally, 0 K).

2. Computational method

First, the geometrical optimisation of distorted perovskite $TbMnO_3$ is performed by using the plane-wave pseudopotential method based on the density functional theory (DFT) with the generalised gradient approximation (GGA) in the scheme of Perdwe *et al.*[19] The valence electrons taken into account for $TbMnO_3$ correspond to $Tb4f^85s^25p^65d^16s^2$, Mn $3d^54s^2$, $O2s^22p^4$, respectively. Ultrasoft Vanderbilt-type pseudopotentials are used. Plane-wave cutoff energy of 340 eV and a 5×4×3 grid of Monkhorst–Pack points have been employed in this study to ensure the convergence of the computed structures and energies. Geometric optimisation is achieved by using convergence thresholds of 1.0×10^{-5} eV/atom for total energy, 0.03 eV/Å (1 Å = 0.1 nm) for maximum force, 0.05 GPa for pressure, and 0.001 Å for maximum displacement. The tolerance in the self-consistent field (SCF) calculation is 1.0×10^{-6} eV/atom. For the calculation of the optical properties, which requires a dense mesh of uniformly distributed k-point, the Brillouin zone integration is performed by using the 8×8×6 grid of Monkhorst–Pack points.

It is known that the optical properties of $TbMnO_3$ are determined by frequency-dependent dielectric function $\varepsilon(\omega) = \varepsilon_1(\omega) + \mathrm{i}\varepsilon_2(\omega)$ that is mainly connected with the electronic structure. The imaginary part $\varepsilon_2(\omega)$ of the dielectric function is calculated from the momentum matrix elements between the occupied and unoccupied electronic states and is given by

$$\varepsilon_2 = \frac{2e^2\pi}{\Omega\varepsilon_0} \sum_{k,v,c} |\langle\varphi_k^{\mathrm{c}}|\boldsymbol{u}\cdot r|\varphi_k^{\mathrm{v}}\rangle|^2 \delta(E_k^{\mathrm{c}} - E_k^{\mathrm{v}} - E), \quad (1)$$

where ω is the light frequency, e is the electronic charge, φ_k^{c} and φ_k^{v} are the conduction band (CB) and the valence band (VB) wave-functions at k point, respectively. The real part $\varepsilon_1(\omega)$ of the dielectric function can be derived from the imaginary part by using the Kramers–Kronig dispersion equation. All other optical constants such as the absorption spectrum, the refractive index, the extinction coefficient, the energy-loss spectrum, and the reflectivity can be derived from $\varepsilon_1(\omega)$ and $\varepsilon_2(\omega)$.[20]

3. Results and discussion

3.1. Crystall structure and geometric optimisation

First, we present the crystal structure characterised by x-ray diffraction analysis, as shown in Fig. 1. There are 20 atoms per unit cell and the lattice parameters are $a = 5.293$ Å, $b = 5.838$ Å, and $c = 7.403$ Å, respectively. The geometric optimisation is completed on the basis of the experimental values[21] and the comparison between the theoretical and experimental constants are listed in Table 1. The results show that the optimised lattices are consistent with the experimental values.

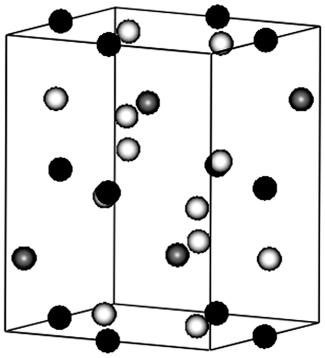


Fig. 1. Crystal structure of orthorhombic distorted perovskite $TbMnO_3$. The black balls are for the Mn element, white balls for the O element and the bigger gray ball for the Tb element.

Table 1. Experimental,[21] and optimised (this work) and previous[22] structural parameters for othorhombic $TbMnO_3$.

lattice constants/Å	experimental value	optimised value	other data
a	5.293	5.396	5.195
b	5.838	5.823	5.758
c	7.403	7.472	7.308

3.2. Band structure and density of states

The calculated energy band structure and the magnified band structure at Fermi level for $TbMnO_3$ are shown in Figs. 2(a) and 2(b), respectively.

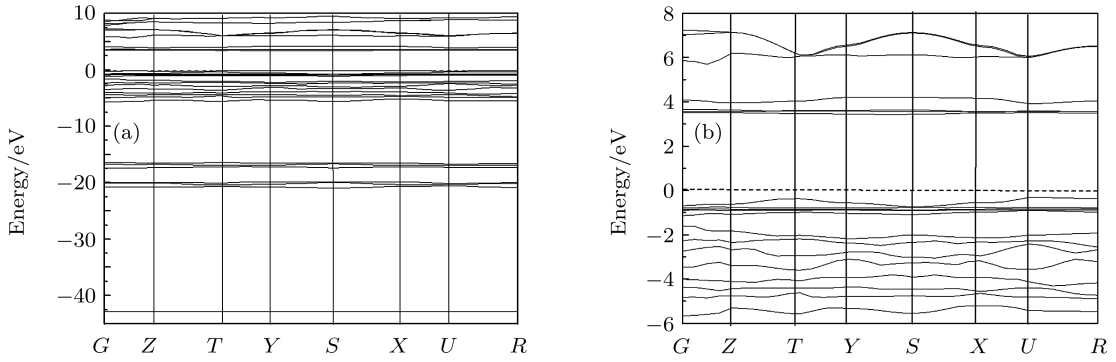


Fig. 2. (a) Band structure of orthorhombic $TbMnO_3$. (b) A magnified view of the band structure around the Fermi level.

The energy band structure, shown in Figs. 3(a) and 3(b) is calculated for the highest number of symmetry points contained in the Brillouin zone, namely along Gamma-*Z*-*T*-*Y*-*S*-*X*-*U*-*R* direction. The Fermi level is located at 0.0 eV. In this paper, noncollinear magnetic structure is neglected because its minor influence on the optical properties of the material. Therefore, we only gave the spin-up states and the scissor operator was selected to be 3.0 eV for a clear separation between the VB and CB states, and the indirect band gap is 3.48 eV, and then true band gap value is 0.48 eV in coincidence with the experimental.[22]

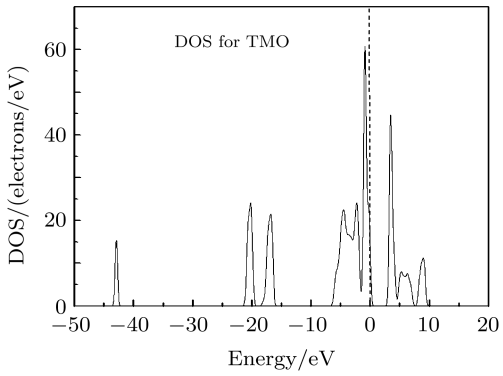


Fig. 3. Total density of states (DOS) of orthorhombic perovskite $TbMnO_3$ (TMO).

To further elucidate the nature of the electronic band structure, the total density of states of $TbMnO_3$ and partial states for Tb, Mn, and O elements are calculated and shown in Figs. 4(a)–4(c). Combining the band structure with the (partial) density of states, we find that at the bottom of the VB, the lowest energy band about –42 eV are mainly occupied by Tb $6s^2$ state. The upside of VB consists of Tb 4f states mixed with Mn 3d states and O 2p states, indicating a strong hybridization among them. Thus, $TbMnO_3$ appears to be some covalent features. Meanwhile, above the Fermi level, the CB is dominated by Tb 4f states in the range of 3.05 eV to 4.40 eV, and Mn 3d states in the region of 3.07 eV to 7.3 eV. In this region, strong mixing also occurs between Tb 4f states and Mn 3d states. Moreover, in the upper region of VB, the width and the number of partial density of states (PDOS) for Mn 3d states and O 2p states are more obvious than that of Tb 4f states, indicating the hybridization of Mn–O is stronger than that of Tb–O.

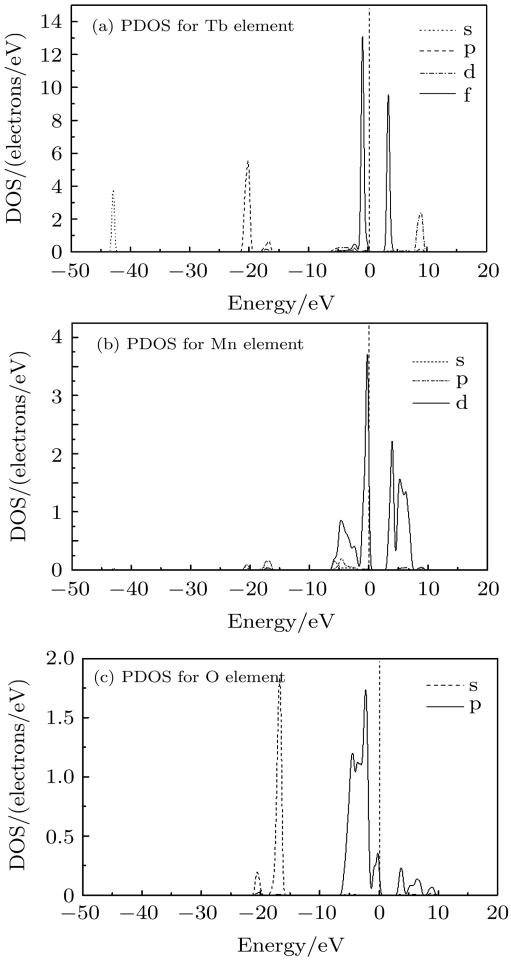


Fig. 4. (a)–(c) The PDOS of Tb, Mn, and O elements, respectively.

3.3. Dielectric and optical properties

The dielectric functions and optical properties of $TbMnO_3$ at equilibrium lattice constants are calculated on the basis of the calculated electronic structure, for the energy range up to 30 eV. The imaginary and real parts of dielectric function are presented in Fig. 5.

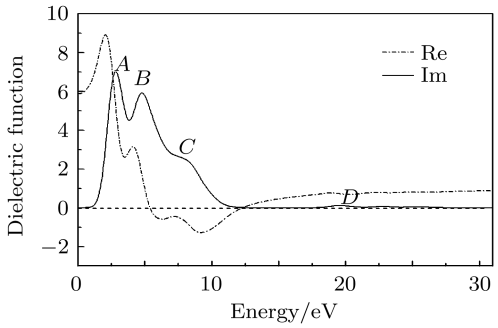


Fig. 5. Calculated imaginary part and real part of the dielectric function for the orthorhombic $TbMnO_3$.

Here, we considered only the incident radiation along direction (100). The imaginary part of dielectric function is directly connected with the transitions from the occupied states to unoccupied states. The absorptive part of dielectric function existed several obvious peaks labeled A, B, C and D, corresponding to the electronic transition between occupied states and unoccupied states. The first peak A (2.82 eV) corresponds mainly to the transitions either from the occupied O 2p to unoccupied Mn 3d states or the d–d transition between Mn 3d states and conduction bands. This peak is very pronounced and higher than other peaks. Peaks B (4.72 eV) and C (7.90 eV) are due to the transitions from the O 2p VB to Mn 3d or Tb 4f higher-energy CB. The last peak D (19.78 eV) is ascribed to the transition of inner electrons from O 2s level to the CB. It should be noted that the peak in $\varepsilon_2(\omega)$ does not imply that the inter-band transition occurs since direct or indirect transitions may also be found in band structure with produced energy corresponding to the same peak.[23] The calculated static dielectric constant $\varepsilon(0)$ was found to be 5.85 eV at the equilibrium lattice constant.

The calculated results on absorption, reflectivity, refractive index and loss function were shown in Figs. 6–9.

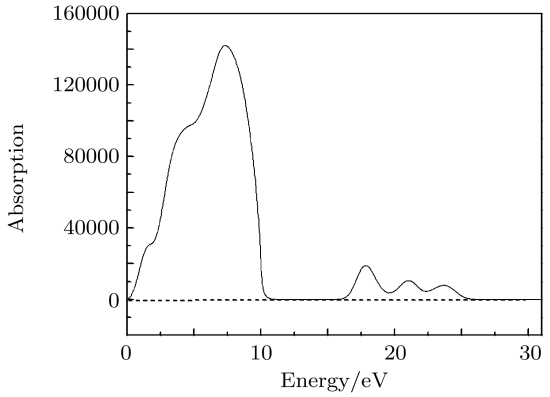


Fig. 6. Calculated absorption spectrum for the distorted $TbMnO_3$.

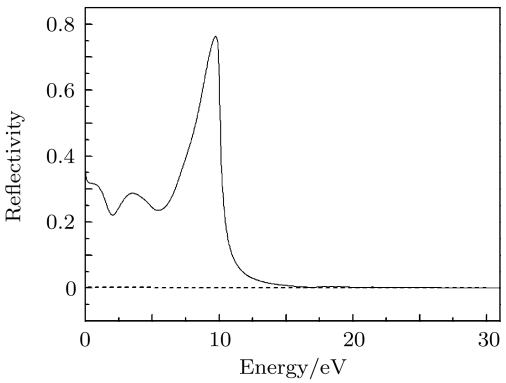


Fig. 7. Calculated reflectivity of distorted $TbMnO_3$.

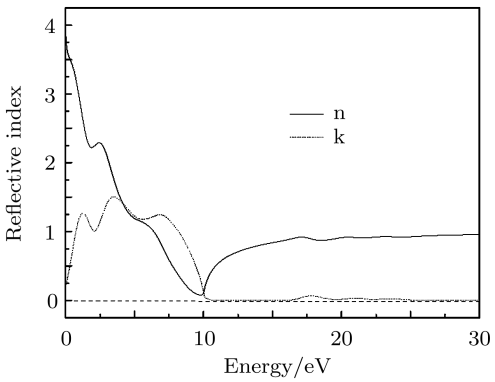


Fig. 8. Calculated complex refractive index for the distorted $TbMnO_3$.

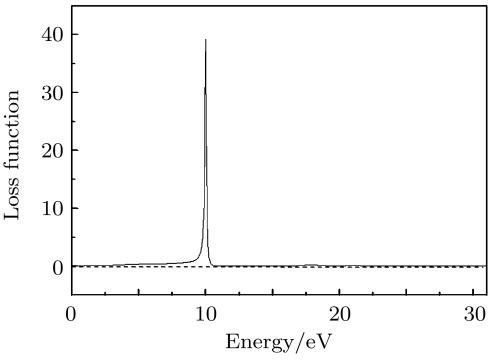


Fig. 9. Calculated loss-spectrum of distorted $TbMnO_3$.

The Gaussian smearing used for calculating the above properties is 0.2 eV. From Fig. 6, one can see that the linear absorption spectrum exists two anomalies before reaching a maximum at 7.2 eV, and then decreased rapidly to zero around 10 eV. Meanwhile, the width of the absorption spectrum in the range of 0 to 10 eV is larger than that of between 15 eV and 25 eV. In the energy range of 0 to 6.5 eV, the reflectivity was lower than 35% and two minima emerge at about 3 eV and 6 eV, respectively, corresponding to the two anomalies in absorption spectra. And the calculated reflectivity reached the maximum value of roughly 78% nearby 10 eV then also decreased rapidly. The refractive index and the extinction coefficient are displayed in Fig. 8. The value of the static refractive index $n(0)$ is found to be 3.6 eV and then decreases gradually to almost zero with increasing the incident energy to 10 eV, although several unnormal values emerge. Then, the refractive index increases a little and becomes nearly constant after 10 eV. Simultaneously, the local minimum of extinction of coefficient $k(\omega)$ also occurs as that of refractive index. The origin of structures in the imaginary part of the dielectric function can be used to explain the structures of refractive index. The energy-loss spectra, shown in Fig. 9, describe the energy-loss of a fast electron traversing in the material. The main peak in loss spectrum is generally defined as the bulk plasma frequency $\omega_{\rm p}$, which occurs when $\varepsilon_2 < 1$ and ε_1 reach the zero point.[24] For $TbMnO_3$, the main peak in loss spectrum at 10 eV corresponds to the abrupt reductions of reflectivity. This process is associated with the transitions from the filled O 2s bands to the empty CB.

4. Conclusions

In summary, we have performed the calculations on the structural parameters, electronic structure and optical properties by first principles using the DFT within GGA method. The calculated lattice parameters are in good agreement with previous calculations and experimental data. The electronic structures of $TbMnO_3$ reveal that the top of the VB are occupied by O 2p, Tb 4f and Mn 3d states, and the bottom of the CB by Tb 4f and Mn 3d states, respectively. Furthermore, the Mn–O bond possesses a stronger covalent bonding strength than that of the Tb–O bond. Finally, the dielectric function, absorption coefficient, reflectivity spectrum, complex refractive index and electron energy-loss are obtained for radiation up to 30 eV. Using the band structure, we discuss the relations of the optical properties to the inter-band transitions. It is found that the orthorhombic distorted perovskite $TbMnO_3$ is a promising dielectric material.

References

[1] Ramesh R and Spaldin N 2007 *Natute Mater.* **6** 21
[2] Tokura Y 2007 *J. Magn. Magn. Mater.* **310** 1145
[3] Zhang Y, Deng C Y, Ma J, Lin Y H and Nan C W 2008 *Chin. Phys.* B **17** 3910
[4] Eerenstein W, Mathur N D and Scott J F 2006 *Nature* **442** 17
[5] Sun Y, Ming X, Meng X, Sun Z H, Lan M, Chen G and Xiang P 2009 *Acta Phys. Sin.* **58** 5653 (in Chinese)
[6] Manuel B and Agnes B 2008 *Natute Mater.* **7** 425
[7] Claude E and Nicola A S 2006 *Curr. Opin. In Solid State and Mater. Sci.* **9** 128
[8] Feng H J and Liu F M 2009 *Chin. Phys.* B **18** 2487
[9] Ge B H, Li F H, Li X M, Wang Y M, Chi Z H and Jin C Q 2008 *Chin. Phys.* B **17** 3163
[10] Zhong C G, Jiang Q, Fang J H and Ge C W 2009 *Acta Phys. Sin.* **58** 3491 (in Chinese)
[11] Quezel S and Tcheou F 1977 *Physica* B **86** 88
[12] Kimura T and Goto T 2003 *Nature* **426** 55
[13] Kenzelmann M and Harris A B 2005 *Phys. Rev. Lett.* **95** 087206
[14] Katsura H and Naoto N 2005 *Phys. Rev. Lett.* **95** 057205
[15] Li C L, Wang H and Wang B 2007 *Appl. Phys. Lett.* **91** 07190
[16] Li C L, Wang B, Wang R and Wang H 2008 *Physica* B **403** 539
[17] Li C L, Wang B, Wang R and Wang H 2008 *Comp. Mate. Sci.* **42** 614
[18] Wang H, Zheng Y and Cai M Q 2009 *Soli. Stat. Comm.* **149** 641
[19] Perdew J P, Burke K and Ernzerhof M 1996 *Phys. Rev. Lett.* **77** 3865
[20] Saha S and Sinha T P 2000 *Phys. Rev.* B **62** 8828
[21] Alonso J A and Martinez-Lope M J 2000 *Inorg. Chem.* **39** 917
[22] Cui Y M, Wang C C and Cao B S 2005 *Soli. Stat. Commun.* **133** 641
[23] Cai M Q, Yin Z and Zhang M S 2003 *Appl. Phys. Lett.* **83** 14
[24] Saniz R and Ye L H 2006 *Phys. Rev.* B **74** 014209